EAI Endorsed Transactions
on Energy Web

Research Article EAI.EU

Electric Vehicle Battery Charging Station based on Bipolar dc Power Grid with Grid-to-Vehicle, Vehicle-to-Grid and Vehicle-to-Vehicle Capabilities

Tiago J. C. Sousa[1,*], Vítor Monteiro[1], Sérgio Coelho[1], Luís Machado[1], Delfim Pedrosa[1] and João L. Afonso[1]

[1]ALGORITMI Research Centre, University of Minho, Guimarães – Portugal

Abstract

An electric vehicle (EV) battery charging station (EV-BCS) based on a bipolar dc power grid is presented in this paper, which is capable of delivering power to the grid (vehicle-to-grid – V2G mode), and directly exchange power between different EVs connected to the EV-BCS (vehicle-to-vehicle – V2V mode), besides the traditional battery charging operation (grid-to-vehicle – G2V mode). The presented EV-BCS is based on three-level bidirectional buck-boost dc-dc converters and has a modular structure. Simulation results are presented with the aim of validating the aforementioned operation modes, being considered two EVs for simplicity reasons, since it is enough to validate the proposed operation modes. The presented results comprise both balanced and unbalanced operation in terms of power from the EVs viewpoint, with the purpose of considering a real scenario of operation, where a balanced consumption or power injection from the bipolar dc power grid side is always guaranteed.

Keywords: Electric Vehicle, Battery Charging Station, Bipolar dc Power Grid, Three-Level dc-dc Converter.

Received on 29 October 2021, accepted on 15 February 2023, published on 16 February 2023

doi: 10.4108/ew.v9i5.3049

*Corresponding author. Email: Tsousa@dei.uminho.pt

1. Introduction

Electric vehicles (EVs) are considered a viable alternative to internal combustion engine vehicles, since they reduce the emission of greenhouse gases from the utilization level point of view, as well as the exploitation of fossil resources [1], [2]. Besides environmental issues, EVs can also have an interesting role regarding smart grids, being combined with renewable energy sources and energy storage systems and rendering ancillary services [3]-[5]. In this regard, the most common operation mode and one of the first ones being proposed was vehicle-to-grid (V2G) [6]-[8], in addition to the primordial battery charging functionality (grid-to-vehicle (G2V)). However, one of the main issues bottlenecking the spread of EVs is the battery charging infrastructure [9], [10]. In the literature can be found some strategies aiming to circumvent this issue, such as battery swapping [11]-[14] and the combination of solar photovoltaic panels and energy storage systems [15]-[17].

As a consequence of fundamental systems for distributed generation and smart grids operating in dc, such as solar photovoltaic panels and energy storage systems, dc power grids are also receiving attention from researchers. The transmission of power in dc can be advantageous over ac, since the former does not present constraints such as harmonic currents, reactive power and skin effect, thereby making dc microgrids an important research topic [18], [19]. Regarding dc power grids, they can either be unipolar or bipolar depending on the number

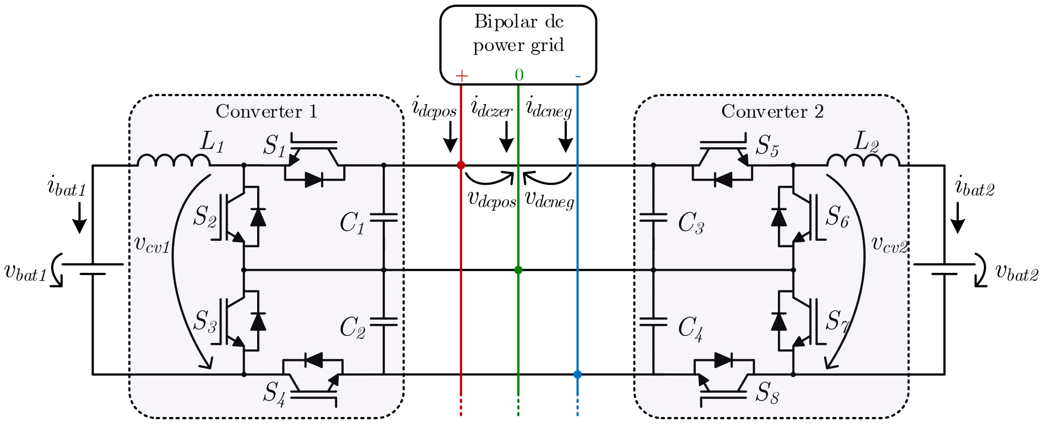

Figure 1. Power structure of the electric vehicle (EV) battery charging station (EV-BCS).

of active conductors. While unipolar dc power grids comprise only one active conductor and neutral, originating a single voltage value, bipolar dc power grids contain two active conductors and neutral, giving rise to two symmetrical voltages referenced to neutral or, additionally, one voltage with the double of the base value. Compared to their unipolar counterpart, bipolar dc power grids are advantageous since they allow two voltage values instead of one, besides being more reliable and presenting a higher energy transmission capacity [20]-[22].

In the literature, the application of bipolar dc power grids in EV-BCSs can be found. For instance, an EV-BCS based on a neutral point clamped ac-dc converter is presented in [23], where a bipolar dc power grid is formed by the split dc-link of this converter topology. The dc-dc converters that control the battery charging are connected to the bipolar dc power grid, despite not being addressed in such publication. References [24]-[27] analyze the use of three-level dc-dc converters in bipolar dc power grid based EV-BCSs, although the V2G operation is not covered. In this sense, this paper presents an EV-BCS based on a bipolar dc power grid that, besides the conventional G2V operation, also comprises V2G. Furthermore, a relatively recent operation mode is also considered in this paper, namely vehicle-to-vehicle (V2V) [28]-[31]. In the scope of this paper, only the operation of the dc-dc converters of the EV-BCS is addressed.

The paper is organized as follows: Section 2 presents the EV-BCS, namely the used power converters and their control; Section 3 presents the simulation model and the obtained results; finally, in Section 4 are presented the main conclusions of the paper.

2. Electric Vehicle Battery Charging Station (EV-BCS)

In this section, the power structure of the EV-BCS is presented, namely the employed dc-dc converter and its respective control system. The referred converter is a three-level two-quadrant buck-boost topology, allowing bidirectional power flow and, consequently, G2V, V2G and V2V operation modes. Moreover, the presence of a split dc-link makes this converter appropriate for bipolar dc power grids [32], [33]. Figure 1 presents the EV-BCS power structure for a number of converters (and EVs) equal to two, where, in theory, any number of equal converters can be connected. It should be referred that only two converters were chosen due to simplicity issues and because it is enough to validate the desired operation modes. In [34], the same power structure is analyzed for smart grids applications, i.e., two three-level two-quadrant buck-boost dc-dc converters sharing the high voltage side.

In the low voltage side, each converter x is connected to an EVx, and, in the high voltage side, to the bipolar dc power grid, where the positive rail voltage (v_{dcpos}) is applied to the upper capacitor (C_{2x-1}) and the negative rail voltage (v_{dcneg}) is inversely applied to the lower capacitor (C_{2x}). Being a bipolar dc power grid, it is true that $v_{dcpos} = -v_{dcneg}$; hence, the high side total voltage is $2v_{dcpos}$. Nevertheless, since the dc-dc converter operates with three voltage levels, each power semiconductor withstands only a maximum voltage of v_{dcpos}.

Regarding buck mode, where power flows from the high voltage side (bipolar dc power grid) to the low voltage side (battery), corresponding to G2V operation, each converter x uses power semiconductors S_{4x-3} and S_{4x} (S_1, S_4 in EV1 and S_5, S_8 in EV2). The voltage produced by each converter x (v_{cvx}) can assume three values (0, v_{dcpos}, $2v_{dcpos}$). In equation (1), the possibilities for v_{cvx} for each switching state can be seen in buck mode, where 0 represents the off-state and 1 the on-state. Equation (2) shows the two operating regions for the converter with respect to the voltages v_{batx} and v_{dcpos} and the duty-cycle (D). In terms of modulation applied to the converters, a phase shift of 180º is used between the two active semiconductors, doubling the v_{cvx} frequency with respect to its switching frequency.

$$v_{cvx} = \begin{cases} 0, & S_{4x-3} = 0,\ S_{4x} = 0 \\ v_{dcpos}\,, & S_{4x-3} = 0(1),\ S_{4x} = 1(0) \\ 2v_{dcpos}\,, & S_{4x-3} = 1,\ S_{4x} = 1 \end{cases} \quad (1)$$

$$\begin{array}{l} \text{If } v_{cvx} < 2v_{dcpos} - v_{batx} \;\rightarrow\; D < 50\%,\, v_{cvx} = \{0,\, v_{dcpos}\}, \\ \text{If } v_{cvx} > 2v_{dcpos} - v_{batx} \;\rightarrow\; D > 50\%,\, v_{cvx} = \{v_{dcpos},\, 2v_{dcpos}\}. \end{array} \quad (2)$$

A predictive current control was used for controlling each EV battery current. According to this strategy, for each time instant k, each converter x should produce a voltage v_{cvx} so that each current i_{batx} follows its reference $i_{batrefx}$. In buck mode, where each current i_{batx} is considered positive, the produced voltage can be calculated as follows:

$$v_{cvx}[k] = v_{batx}[k] + L_x f_s \left(i_{batrefx}[k] - i_{batx}[k]\right), \quad i_{batrefx} > 0, \quad (3)$$

where L_x is the inductance value of dc-dc converter x inductor and f_s is the digital control system sampling frequency.

Regarding boost mode, where power flows from the low voltage side (battery) to the high voltage side (bipolar dc power grid), corresponding to V2G operation, each converter x uses power semiconductors S_{4x-2} and S_{4x-1} (S_2, S_3 in EV1 and S_6, S_7 in EV2). The voltage produced by each converter x (v_{cvx}) can also assume three values (0, v_{dcpos}, $2v_{dcpos}$). In equation (4), the possibilities for v_{cvx} can be seen for each switching state in boost mode, where 0 represents the off-state and 1 the on-state. Equation (5) shows the two operating regions for the converter with respect to the voltages v_{batx} and v_{dcpos} and the duty-cycle (D). In terms of modulation applied to the converters, similarly to buck mode, a phase shift of 180º is used between the two active semiconductors, doubling the v_{cvx} frequency with respect to its switching frequency.

$$v_{cvx} = \begin{array}{ll} 0, & S_{4x-2} = 1,\, S_{4x-1} = 1 \\ v_{dcpos}\,, & S_{4x-2} = 1(0),\, S_{4x-1} = 0(1) \\ 2v_{dcpos}\,, & S_{4x-2} = 0,\, S_{4x-1} = 0 \end{array} \quad (4)$$

$$\begin{array}{l} \text{If } v_{cvx} > 2v_{dcpos} - v_{batx} \;\rightarrow\; D > 50\%,\, v_{cvx} = \{0,\, v_{dcpos}\}, \\ \text{If } v_{cvx} < 2v_{dcpos} - v_{batx} \;\rightarrow\; D < 50\%,\, v_{cvx} = \{v_{dcpos},\, 2v_{dcpos}\}. \end{array} \quad (5)$$

The predictive current control is also used in boost mode, in this case with the current i_{batx} assuming negative values. For positive values of $i_{batrefx}$, the digital implementation of this current control is given as follows:

$$v_{cvx}[k] = v_{batx}[k] - L_x f_s \left(i_{batrefx}[k] + i_{batx}[k]\right), \quad i_{batrefx} > 0. \quad (6)$$

3. Computational Simulations

This section presents the simulation model and results of the EV-BCS for two EVs, being addressed the G2V, V2G and V2V operation modes, as well as a combination of V2V with G2V and V2V with V2G. The computational simulations were performed in the software PSIM v9.1 from Powersim. The adopted battery model, which is the Thevenin model, can be seen in Figure 2, comprised by the open-circuit voltage (v_{ocx}), a capacitor to emulate the dynamic behavior of the battery (C_{batx}), a parallel resistor to emulate the battery self-discharge (R_{px}) and a series resistor that represents the internal resistance of the battery (R_{sx}). Table 1 presents the parameters of the power converter and batteries of each EV (where it can be seen that the converters are equal), as well as the batteries, presenting different initial voltage values in order to emulate a more realistic scenario, with v_{bat1} starting with 250 V and v_{bat2} with 200 V.

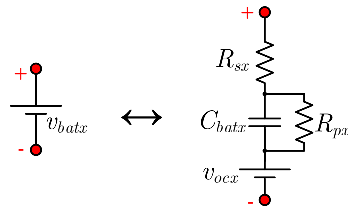

Figure 2. Thevenin battery model for each EV*x*.

Table 1. Simulation parameters of the EV-BCS and EV batteries.

Parameter	Value
Initial v_{bat1}	250 V
Initial v_{bat2}	200 V
v_{ocx}	150 V
C_{batx}	0.5 F
R_{sx}	0.1 Ω
R_{px}	100 kΩ
L_x	500 µH
C_{2x-1}, C_{2x}	100 µF
v_{dcpos}	200 V
v_{dcneg}	-200 V
dc power grid impedance	0.1 Ω, 10 µH
Switching frequency	50 kHz
Sampling frequency	50 kHz

Figure 3 shows the usual operation of both EVs at a charging station (G2V), both charging their batteries with the same current value (20 A). The figure shows the battery voltages (v_{bat1} and v_{bat2}) and currents (i_{bat1} and i_{bat2}), the currents drawn from the dc power grid, namely in the positive rail (i_{dcpos}), neutral rail (i_{dczer}) and negative rail (i_{dcneg}), and the voltages produced by the converters (v_{cv1} and v_{cv2}). It can be seen that the battery voltages are slightly higher than their original values (2 V higher), which is due to the internal resistance of the batteries and not due to the energy accumulation process, given that the figure initial instant is 2 ms. It can be seen that both battery currents present the same average value of 20 A, but i_{bat2} presents a much smaller ripple than i_{bat1}. This is due to the fact that the voltage v_{bat2} is practically half (202 V) the total dc power grid voltage, making the three-level buck-boost dc-dc converter operate in a region of strong ripple cancelling. This is visible in the voltage produced by this converter (v_{cv2}), presenting a very low duty-cycle between voltage levels 200 V and 400 V (in other words, presenting a duty-cycle slightly higher than 50%). It is noticeable from voltage v_{cv1} that converter 1 operates with the same voltage levels but with a higher duty-cycle, meaning a higher ripple in i_{bat1}. Regarding the currents absorbed from the dc power grid, it can be seen that i_{dcpos} and i_{dcneg} are symmetrical, with average values of 23 A and -23 A, respectively, the first one being positive and the second being negative, meaning that the dc power grid is providing power. The current i_{dczer} is the negative sum of i_{dcpos} and i_{dcneg}, therefore presenting a null average value.

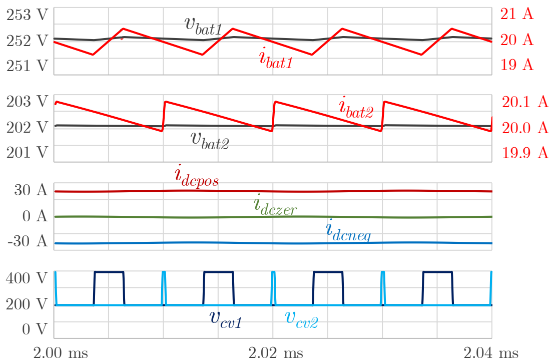

Figure 3. Simulation results of the G2V operation mode when EV1 and EV2 are charging with a current of 20 A.

Figure 4 shows the operation of both EVs in G2V but with different current values in order to simulate an unbalance situation. EV1 is charging with a current of 20 A, while EV2 is charging with a current of 40 A. The figure shows v_{bat1}, v_{bat2}, i_{bat1}, i_{bat2}, i_{dcpos}, i_{dczer}, i_{dcneg}, v_{cv1} and v_{cv2}. In this case, v_{bat2} presents a value of 204 V, showing the effect of the battery internal resistance when higher currents are applied. It can be seen that both i_{bat1} and i_{bat2} present the expected average value, with EV1 presenting the same results as the previous case. Despite being a higher current, i_{bat2} still has a low ripple due to the same reason as previously mentioned, as it can be seen from voltages v_{cv1} and v_{cv2}. Regarding the currents absorbed from the dc power grid, i_{dcpos} and i_{dcneg} are symmetrical but with a higher average value than previously (33.6 A), also with the first one being positive and the second being negative. Accordingly, i_{dczer} has no average value. Based on this result, it can be perceived that the EV-BCS is able to consume balanced currents from the bipolar dc power grid even with unbalanced battery charging operation.

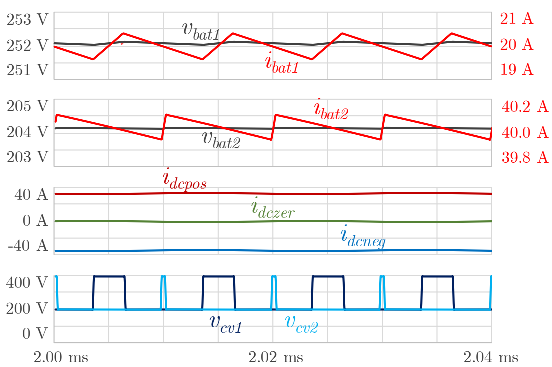

Figure 4. Simulation results of the G2V operation mode when EV1 is charging with a current of 20 A and EV2 is charging with a current of 40 A.

After being presented the G2V operation, both balanced and unbalanced, Figure 5 shows the V2G operation mode for both EVs, discharging their batteries with the same current value (20 A). This figure shows the same variables as the previous ones. It can be seen that both battery currents are negative, meaning that the power flows from the batteries to the dc power grid, as expected in the V2G operation mode. Also, both i_{bat1} and i_{bat2}present the same average value of -20 A, but i_{bat2} presents a much smaller ripple than i_{bat1}, which is due to the same reason as aforementioned. In this case, v_{cv2} presents a very high duty-cycle between voltage levels 0 V and 200 V (in other words, presenting a duty-cycle slightly smaller than 50%). This happens due to the internal resistance of the batteries, which decreases the battery voltage when current is being supplied by the battery, as it can be seen by the 198 V v_{bat2} value, which is lower than half the total dc power grid voltage. Once again, it can be seen that the dc power grid currents i_{dcpos} and i_{dcneg} are symmetrical, but with i_{dcpos} being negative and i_{dcneg} being positive, conversely to the previous cases. This means that the dc power grid is not supplying power but receiving instead, as supposed with the V2G operation mode. The average value of these currents is 22.1 A, with the current i_{dczer} presenting a null average value.

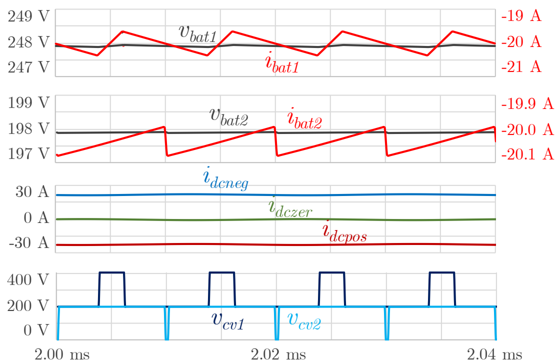

Figure 5. Simulation results of the V2G operation mode when EV1 and EV2 are discharging with a current of 20 A.

Figure 6 shows the operation of both EVs in V2G but with different current values in order to simulate an unbalance situation. EV1 is discharging with a current of 20 A, while EV2 is discharging with a current of 40 A. This figure shows the same variables as the previous ones. As previously, both i_{bat1} and i_{bat2} are negative, meaning that the power flows from the batteries to the dc power grid, as supposed to happen in the V2G operation mode. Both i_{bat1} and i_{bat2} present the expected average value, with EV1 presenting the same results as the previous scenario. In this case, v_{bat2} presents a value of 196 V, showing the effect of the battery internal resistance when higher currents are drawn from the battery. Despite being a higher current, i_{bat2} still has a low ripple due to the same reason as previously mentioned, as it can be seen from voltages v_{cv1} and v_{cv2}. Regarding the dc power grid currents, it is noticeable that i_{dcpos} is negative and i_{dcneg} is positive, as in the previous case, meaning that the dc power grid is receiving power instead of supplying it. Moreover, these currents are symmetrical, presenting an average value of 31.5 A and, therefore, the current i_{dczer} has a null average value. Hence, this result shows that the EV-BCS is able to handle unbalances in the power injected by the EVs without unbalancing the dc power grid currents.

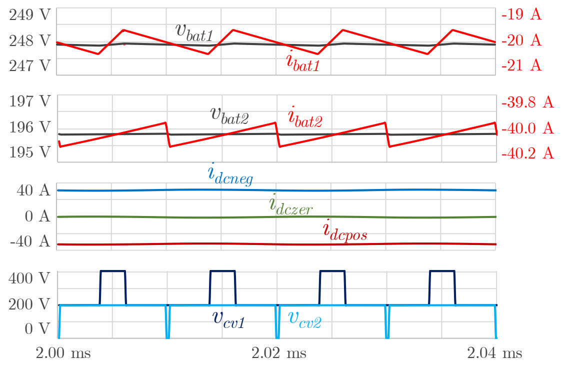

Figure 6. Simulation results of the V2G operation mode when EV1 is discharging with a current of 20 A and EV2 is discharging with a current of 40 A.

After being analyzed the operation modes G2V and V2G, Figure 7 shows the V2V operation mode, where EV1 provides power to EV2. EV2 is charging with a current of 20 A, while EV1 provides the necessary current to perform the battery charging of EV2 without using additional power from the dc power grid. This figure shows the same variables as the previous ones. In this operation mode, i_{bat1} is negative, as happens in V2G, but i_{bat2} is positive, as happens in G2V. It can be seen that i_{bat2} has the expected average value of 20 A, with i_{bat1} presenting an average value of approximately -16.3 A. This difference is due to the voltage mismatch between the battery voltages of both EVs so that the input and output powers are approximately equal. In this case, the voltage v_{bat2} has a value of 202 V, making the produced voltage v_{cv2} alternate between voltage levels 200 V and 400 V. Regarding the dc power grid currents, it can be seen that i_{dcpos} and i_{dcneg} are overlapped and present a null average value, meaning that the dc power grid is neither receiving nor providing power. The current i_{dczer} presents a similar waveform and, as in the previous cases, has no average value.

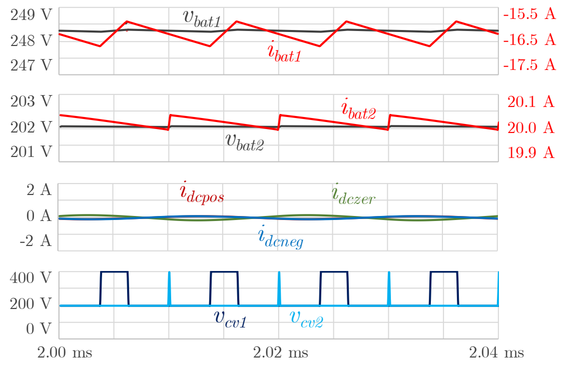

Figure 7. Simulation results of the V2V operation mode when EV1 is discharging with a current of 16.3 A and EV2 is charging with a current of 20 A.

After being addressed the V2V operation mode exclusively, Figure 8 shows the combination of V2V and G2V operation modes, where EV1 provides power to EV2, but the power provided by EV1 is not enough to perform the battery charging of EV2. EV1 is discharging with a current of 20 A, while EV2 is charging with a current of 40 A. This figure shows the same variables as the previous ones. Once again, i_{bat1} is negative, similar to V2G, but i_{bat2} is positive, similar to G2V. Regarding the dc power grid currents, it can be seen that i_{dcpos} is positive and i_{dcneg} is negative, meaning that the dc power grid is providing power. However, the average value of these currents is only 8 A, since the dc power grid only provides the power difference between the power required by EV2 and the power supplied by EV1. As previously, the currents i_{dcpos} and i_{dcneg} are symmetrical, with i_{dczer} presenting a null average value.

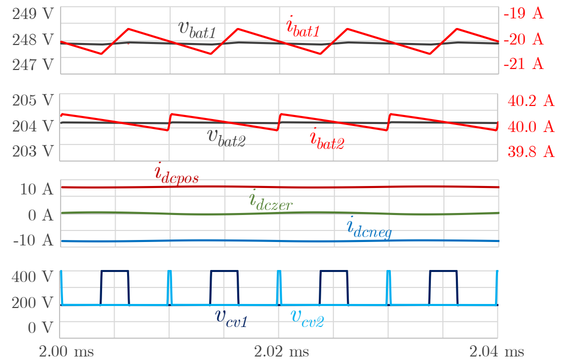

Figure 8. Simulation results of the combination of V2V and G2V operation modes when EV1 is discharging with a current of 20 A and EV2 is charging with a current of 40 A.

Figure 9 shows the combination of V2V and V2G operation modes, where EV1 provides power to EV2, but the power provided by EV1 is more than the power required to perform the battery charging of EV2. EV1 is discharging with a current of 40 A, while EV2 is charging with a current of 20 A. This figure shows the same variables as the previous ones. Once again, i_{bat1} is negative, similar to V2G, but i_{bat2} is positive, similar to G2V. Regarding the dc power grid currents, it can be seen that i_{dcpos} is negative and i_{dcneg} is positive, contrarily to the previous case, meaning that the dc power grid is receiving power. The average value of these currents is only 14.4 A, since the dc power grid only receives the power difference between the power supplied by EV1 the power required by EV2. As in the previous case, the currents i_{dcpos} and i_{dcneg} are symmetrical, with i_{dczer} presenting a null average value.

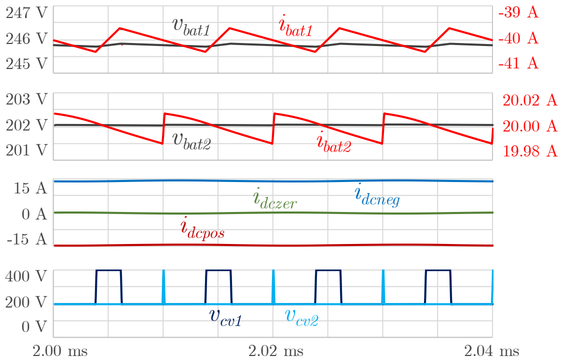

Figure 9. Simulation results of the combination of V2V and V2G operation modes when EV1 is discharging with a current of 40 A and EV2 is charging with a current of 20 A.

In order to provide an overview of the obtained simulation results, Table 2 shows the average values of the main variables for each case, i.e., i_{bat1}, i_{bat2} and i_{dcpos}. The average values of i_{dcneg} and i_{dczer} are not presented since the average value of i_{dcneg} is always symmetrical with respect to i_{dcpos}, while the average value of i_{dczer} is always null, as expected and previously explained.

Table 2. Average value of the currents obtained in the simulation results.

Case	I_{bat1}	I_{bat2}	I_{dcpos}
Balanced G2V (Figure 3)	20 A	20 A	23 A
Unbalanced G2V (Figure 4)	20 A	40 A	33.6 A
Balanced V2G (Figure 5)	-20 A	-20 A	-22.1 A
Unbalanced V2G (Figure 6)	-20 A	-40 A	-31.5 A
V2V (Figure 7)	-16.3 A	20 A	0 A
V2V + G2V (Figure 8)	-20 A	40 A	8 A
V2V + V2G (Figure 9)	-40 A	20 A	-14.4 A

4. Conclusions

This paper presented an electric vehicle (EV) battery charging station (EV-BCS) based on a bipolar dc power grid with vehicle-to-grid (V2G) and vehicle-to-vehicle (V2V) capability, besides the traditional battery charging operation mode (grid-to-vehicle – G2V). The presented EV-BCS is modular and uses three-level bidirectional dc-dc converters. In order to validate all the operation modes (G2V, V2G and V2V, as well as the combination of V2V with G2V and V2G), a case scenario with two converters, and thus two EVs, was considered, being analyzed both balanced and unbalanced operation from the EVs side, in order to emulate a real operation scenario and validate the proper operation of the EV-BCS. The obtained results, based on computational simulations, verify the correct operation of the EV-BCS in all cases, both with balanced and unbalanced current consumption from the EVs, but always with balanced currents from the bipolar dc power grid side.

Acknowledgements.

This work has been supported by FCT – Fundação para a Ciência e Tecnologia within R&D Units Project Scope: UIDB/00319/2020. This work has been supported by the FCT Project DAIPESEV PTDC/EEI-EEE/30382/2017, and by FCT Project newERA4GRIDs PTDC/EEI EEE/30283/2017. Mr. Tiago J. C. Sousa is supported by the doctoral scholarship SFRH/BD/134353/2017 granted by the Portuguese FCT agency.

References

[1] C. C. Chan and Y. S. Wong, "Electric vehicles charge forward," *IEEE Power and Energy Magazine*, vol. 2, no. 6, pp. 24–33, Nov. 2004.

[2] J. Milberg and A. Schlenker, "Plug into the Future," *IEEE Power and Energy Magazine*, vol. 9, no. 1, pp. 56–65, Jan. 2011.

[3] J. Ansari, A. Gholami, A. Kazemi, and M. Jamei, "Environmental/economic dispatch incorporating renewable energy sources and plug-in vehicles," *IET Generation, Transmission & Distribution*, vol. 8, no. 12, pp. 2183–2198, Dec. 2014.

[4] K. Knezovic, S. Martinenas, P. B. Andersen, A. Zecchino, and M. Marinelli, "Enhancing the Role of Electric Vehicles in the Power Grid: Field Validation of Multiple Ancillary Services," *IEEE Transactions on Transportation Electrification*, vol. 3, no. 1, pp. 201–209, 2017.

[5] H. N. T. Nguyen, C. Zhang, and J. Zhang, "Dynamic Demand Control of Electric Vehicles to Support Power Grid With High Penetration Level of Renewable Energy," *IEEE Transactions on Transportation Electrification*, vol. 2, no. 1, pp. 66–75, Mar. 2016.

[6] W. Kempton and J. Tomić, "Vehicle-to-grid power implementation: From stabilizing the grid to supporting large-scale renewable energy," *Journal of Power Sources*, vol. 144, no. 1, pp. 280–294, 2005.

[7] M. Kesler, M. C. Kisacikoglu, and L. M. Tolbert, "Vehicle-to-Grid Reactive Power Operation Using Plug-In Electric Vehicle Bidirectional Offboard Charger," *IEEE Transactions on Industrial Electronics*, vol. 61, no. 12, pp. 6778–6784, Dec. 2014.

[8] V. Monteiro, J. G. Pinto, and J. L. Afonso, "Operation Modes for the Electric Vehicle in Smart Grids and Smart Homes: Present and Proposed Modes," *IEEE Transactions on Vehicular Technology*, vol. 65, no. 3, pp. 1007–1020, Mar. 2016.

[9] Z. Moghaddam, I. Ahmad, D. Habibi, and Q. V. Phung, "Smart Charging Strategy for Electric Vehicle Charging Stations," *IEEE Transactions on Transportation Electrification*, vol. 4, no. 1, pp.76–88, Mar. 2018.

[10] T. Morstyn, C. Crozier, M. Deakin, and M. D. McCulloch, "Conic Optimization for Electric Vehicle Station Smart Charging With Battery Voltage Constraints," *IEEE*

Transactions on Transportation Electrification, vol. 6, no. 2, pp.478–487, Jun. 2020.
[11] Q. Dai, T. Cai, S. Duan, and F. Zhao, "Stochastic modeling and forecasting of load demand for electric bus battery-swap station," *IEEE Transactions on Power Delivery*, vol. 29, no. 4, pp.1909–1917, 2014.
[12] X. Tan, G. Qu, B. Sun, N. Li, and D. H. K. Tsang, "Optimal Scheduling of EV-BCS Serving Electric Vehicles Based on Battery Swapping," *IEEE Transactions on Smart Grid*, vol. 10, no. 2, pp.1372–1384, Mar. 2019.
[13] X. Liu, T. Zhao, S. Yao, C. B. Soh, and P. Wang, "Distributed Operation Management of Battery Swapping-Charging Systems," *IEEE Transactions on Smart Grid*, vol. 10, no. 5, pp.5320–5333, Sep. 2019.
[14] F. Ahmad, M. Saad Alam, I. Saad Alsaidan, and S. M. Shariff, "Battery swapping station for electric vehicles: opportunities and challenges," *IET Smart Grid*, vol. 3, no. 3, pp.280–286, Jun. 2020.
[15] M. Vasiladiotis and A. Rufer, "A Modular Multiport Power Electronic Transformer With Integrated Split Battery Energy Storage for Versatile Ultrafast EV Charging Stations," *IEEE Transactions on Industrial Electronics*, vol. 62, no. 5, pp.3213–3222, May 2015.
[16] Q. Yan, B. Zhang, and M. Kezunovic, "Optimized Operational Cost Reduction for an EV Charging Station Integrated With Battery Energy Storage and PV Generation," *IEEE Transactions on Smart Grid*, vol. 10, no. 2, pp.2096–2106, Mar. 2019.
[17] Y. Deng, Y. Zhang, and F. Luo, "Operational Planning of Centralized Charging Stations Using Second-Life Battery Energy Storage Systems," *IEEE Transactions on Sustainable Energy*, vol. 3029, no. c, pp.1–1, 2020.
[18] B. T. Patterson, "DC, Come Home: DC Microgrids and the Birth of the 'Enernet,'" *IEEE Power and Energy Magazine*, vol. 10, no. 6, pp.60–69, 2012.
[19] D. Kumar, F. Zare, and A. Ghosh, "DC Microgrid Technology: System Architectures, AC Grid Interfaces, Grounding Schemes, Power Quality, Communication Networks, Applications, and Standardizations Aspects," *IEEE Access*, vol. 5, pp.12230–12256, 2017.
[20] L. Sun, F. Zhuo, F. Wang, and T. Zhu, "A Nonisolated Bidirectional Soft-Switching Power-Unit-Based DC–DC Converter With Unipolar and Bipolar Structure for DC Networks Interconnection," *IEEE Transactions on Industry Applications*, vol. 54, no. 3, pp.2677–2689, May 2018.
[21] L. Guo, G. Yao, C. Huang, and L. Zhou, "Bipolar output direct-coupled DC–DC converter applied to DC grids," *The Journal of Engineering*, vol. 2019, no. 16, pp.1474–1479, Mar. 2019.
[22] C. Perera, J. Salmon, and G. J. Kish, "Multiport Converter with Independent Control of AC and DC Power Flows for Bipolar DC Distribution," *IEEE Transactions on Power Electronics*, vol. 8993, no. c, pp.1–1, 2020.
[23] S. Rivera, B. Wu, S. Kouro, V. Yaramasu, and J. Wang, "Electric Vehicle Charging Station Using a Neutral Point Clamped Converter With Bipolar DC Bus," *IEEE Transactions on Industrial Electronics*, vol. 62, no. 4, pp.1999–2009, Apr. 2015.
[24] L. Tan, B. Wu, V. Yaramasu, S. Rivera, and X. Guo, "Effective Voltage Balance Control for Bipolar-DC-Bus-Fed EV Charging Station With Three-Level DC–DC Fast Charger," *IEEE Transactions on Industrial Electronics*, vol. 63, no. 7, pp.4031–4041, Jul. 2016.
[25] L. Tan, B. Wu, S. Rivera, and V. Yaramasu, "Comprehensive DC Power Balance Management in High-Power Three-Level DC–DC Converter for Electric Vehicle Fast Charging," *IEEE Transactions on Power Electronics*, vol. 31, no. 1, pp.89–100, Jan. 2016.
[26] S. Rivera and B. Wu, "Electric Vehicle Charging Station With an Energy Storage Stage for Split-DC Bus Voltage Balancing," *IEEE Transactions on Power Electronics*, vol. 32, no. 3, pp.2376–2386, Mar. 2017.
[27] S. Kim, H. Cha, and H.-G. Kim, "High-Efficiency Voltage Balancer Having DC–DC Converter Function for EV Charging Station," *IEEE Journal of Emerging and Selected Topics in Power Electronics*, vol. 6777, no. c, pp.1–1, 2019.
[28] T. J. C. Sousa, V. Monteiro, J. C. A. Fernandes, C. Couto, A. A. N. Melendez, and J. L. Afonso, "New Perspectives for Vehicle-to-Vehicle (V2V) Power Transfer," *in IECON 2018 - 44th Annual Conference of the IEEE Industrial Electronics Society*, 2018, pp. 5183–5188.
[29] S. Taghizadeh, P. Jamborsalamati, M. J. Hossain, and J. Lu, "Design and Implementation of an Advanced Vehicle-to-Vehicle (V2V) Power Transfer Operation Using Communications," *in 2018 IEEE International Conference on Environment and Electrical Engineering and 2018 IEEE Industrial and Commercial Power Systems Europe (EEEIC / I&CPS Europe)*, 2018, pp. 1–6.
[30] X. Mou, R. Zhao, and D. T. Gladwin, "Vehicle to vehicle charging (V2V) bases on wireless power transfer technology," *in IECON 2018 - 44th Annual Conference of the IEEE Industrial Electronics Society*, 2018, pp. 4862–4867.
[31] X. Mou, "Vehicle-to-Vehicle charging system fundamental and design comparison," in *2019 IEEE International Conference on Industrial Technology (ICIT)*, 2019, pp. 1628–1633.
[32] M. Shen, F. Z. Peng, and L. M. Tolbert, "Multilevel DC–DC Power Conversion System With Multiple DC Sources," *IEEE Transactions on Power Electronics*, vol. 23, no. 1, pp.420–426, Jan. 2008.
[33] M. Yilmaz and P. T. Krein, "Review of Battery Charger Topologies, Charging Power Levels, and Infrastructure for Plug-In Electric and Hybrid Vehicles," *IEEE Transactions on Power Electronics*, vol. 28, no. 5, pp. 2151–2169, May 2013.
[34] V. Monteiro, T. J. C. Sousa, M. J. Sepúlveda, C. Couto, A. Lima, J. L. Afonso, "A Proposed Bidirectional Three Level dc-dc Power Converter for Applications in Smart Grids: An Experimental Validation", in *2019 IEEE SEST International Conference on Smart Energy Systems and Technologies*, Porto, Portugal, Sept. 2019.